

ANALYSIS OF BIOFUELS REACTING FLOWS IN DUCTS

Vinicius M. Sauer, vsauer@ufrj.br

Albino J. K. Leiroz, leiroz@mecanica.ufrj.br

Marcelo J. Colaço, colaco@mecanica.ufrj.br

Federal University of Rio de Janeiro

Department of Mechanical Engineering

PO Box 68503 - Rio de Janeiro, RJ, Brazil - 21941-972

Abstract. *The present work describes a confined axisymmetric reactive flow in a cylindrical duct. The fuels considered in the analysis are methane and ethanol, with ambient air as oxidant. The thermodynamical and transport properties are admitted dependent on temperature. Finite Volume Method is used to solve the conservation equations and the SIMPLEC algorithm is used to consider velocity-pressure coupling. Chemical reactions are treated with flame sheet model, being the reaction mechanism expressed by an irreversible infinitely fast one step global reaction. Results show a general behavior of the combustion system. The obtained profiles for methane and ethanol flames are compared.*

Keywords: *Flame-sheet model, confined laminar diffusion flame, finite volume method*

1. NOMENCLATURE

c_p	constant pressure specific heat
\mathcal{D}	mass diffusion coefficient
g	gravitational constant
h_{RP}	enthalpy of reaction
F	fuel
O	oxidizer
p	pressure
r	radial coordinate
t	time
T	temperature
u	axial velocity
v	radial velocity
W	molecular weight
x	axial coordinate

Y	mass fraction
Z	mixture fraction

Greek Symbols

μ	viscosity
ν	stoichiometric coefficient
ρ	specific mass

Subscripts

0	reference state
A_∞	air inlet
F	fuel
F_∞	fuel inlet
N	inert gas
O	oxidizer
P	products

2. INTRODUCTION

Diffusion flames have an important position in practical applications since many combustion systems utilize this kind of flame, also named non-premixed Williams (1994), in the presence of turbulent flows. The term diffusion flame was introduced by Burke and Schumann (1928) to designate flames in which fuel and oxidant are initially separated, mixing in a region where combustion occurs, forming a flame surface.

The experimental analysis of a confined axisymmetric methane laminar flame presented by Mitchell *et al.* (1980) has been used for years as a reference to the development of new experiments and to the validation of numerical solutions. Keyes and Smooke (1987) utilized the flame sheet model as a starting estimate for counterflow diffusion flame problem. They obtained a numerical solution for boundary layer equations and validated it using the experimental results of Mitchell *et al.* (1980). Xu and Smooke (1993) applied a primitive variable Newton's Method for the calculation of an axisymmetric laminar diffusion flame based on the experiment of Mitchell *et al.* (1980). Ern *et al.* (1995) used the velocity-vorticity

formulation and Riedel (1998) applied a solution obtained using the finite volume method with unstructured grid to analyze the same system (Mitchell *et al.*, 1980). More recently, Tarhan and Selçuk (2003) applied the method of lines to the numerical simulation of a confined methane/air laminar diffusion flame, extended by Uygur *et al.* (2006) and also Uygur *et al.* (2008) that presented a solution considering thermal radiation; all of them also based on the experiment of Mitchell *et al.* (1980).

The literature of ethanol flames is more restricted. Lyu and Chen (1991) used ethanol to the solution of a non-confined diffusion flame obtained by the fuel vaporization on the walls of a cylinder and on a flat plate, considering boundary layer approximation. Saxena and Williams (2007) presented the numerical and experimental solution of a counterflow ethanol diffusion flame. The numerical solution was obtained using of a commercial software that considered several effects, like radiation heat transfer, the Soret effect, multicomponent diffusion and a detailed reaction mechanism.

The present work describes a confined flame based on two different fuels: methane and ethanol. Conservation equations are considered by the use of the finite volume method and variable properties. The flame-sheet method is used to simplify the chemical reactions of the system. The results of the methane and ethanol flame are compared and analyzed.

3. MATHEMATICAL MODELING

Reactive flows in multicomponent systems are governed by four conservation laws. These laws are mathematically represented by the equation of continuity, equation of species, equation of moment and equation of energy. The flame-sheet model is used to simplify this set of equations, namely, by considering Lewis Number equals to one, resulting in a conserved scalar conservation equation.

In diffusion-type flames, the burning rate is controlled by the rate at which fuel and oxidizer are brought together in proper proportions (Tarhan and Selçuk, 2003). In flame-sheet model the chemical reactions are described by a single one-step irreversible reaction corresponding to the infinitely fast conversion of reactants into stable products, assumed to be limited to a very thin exothermic reaction zone located at the locus of the stoichiometric mixing of fuel and oxidizer, where temperature and the products of combustion are maximized (Keyes and Smooke, 1987). This assumption results in the absence of fuel in the oxidizer side and of oxidizer in the fuel side. In the presence of inter gas (N), the overall irreversible reaction of fuel (F) and oxidizer (O) to form product (P) can be written as



where ν_F , ν_O , ν_N and ν_P are the stoichiometric coefficients of each species. To further simplify the governing equations it is assumed that thermal diffusion is negligible, the specific heats of all species are constant and diffusion velocities obey Fick's law. The equation of continuity, equation of moment in axial and radial directions and conserved scalar conservation equations are given, respectively, in cylindrical coordinates system, by

$$\frac{\partial \rho}{\partial t} + \frac{1}{r} \frac{\partial}{\partial x}(\rho r u) + \frac{1}{r} \frac{\partial}{\partial r}(\rho r v) = 0 \quad (2)$$

$$\begin{aligned} \frac{\partial}{\partial t}(\rho u) + \frac{1}{r} \frac{\partial}{\partial x}(\rho r u u) + \frac{1}{r} \frac{\partial}{\partial r}(\rho r v u) = -\frac{\partial p}{\partial x} + \frac{1}{r} \frac{\partial}{\partial x} \left(r \mu \frac{\partial u}{\partial x} \right) + \frac{1}{r} \frac{\partial}{\partial r} \left(r \mu \frac{\partial u}{\partial r} \right) + \frac{1}{r} \frac{\partial}{\partial r} \left(r \mu \frac{\partial v}{\partial x} \right) + \\ + \frac{1}{3} \frac{1}{r} \frac{\partial}{\partial x} \left(r \mu \frac{\partial u}{\partial x} \right) - \frac{2}{3} \frac{1}{r} \frac{\partial}{\partial x} \left[\mu \frac{\partial}{\partial r} (r v) \right] + \rho g \end{aligned} \quad (3)$$

$$\begin{aligned} \frac{\partial}{\partial t}(\rho v) + \frac{1}{r} \frac{\partial}{\partial x}(\rho r u v) + \frac{1}{r} \frac{\partial}{\partial r}(\rho r v v) = -\frac{\partial p}{\partial r} + \frac{1}{r} \frac{\partial}{\partial x} \left(r \mu \frac{\partial v}{\partial x} \right) + \frac{1}{r} \frac{\partial}{\partial r} \left(r \mu \frac{\partial v}{\partial r} \right) + \frac{1}{r} \frac{\partial}{\partial r} \left(r \mu \frac{\partial u}{\partial r} \right) + \\ + \frac{1}{r} \frac{\partial}{\partial x} \left(r \mu \frac{\partial u}{\partial r} \right) - \frac{2}{3} \frac{1}{r} \frac{\partial}{\partial r} \left[\mu \frac{\partial}{\partial r} (r v) \right] - \frac{2}{3} \frac{1}{r} \frac{\partial}{\partial r} \left[r \mu \frac{\partial u}{\partial x} \right] - \frac{2 \mu v}{r^2} + \frac{2}{3} \frac{\mu}{r^2} \frac{\partial}{\partial r} (r v) + \frac{2}{3} \frac{\mu}{r} \frac{\partial u}{\partial x} \end{aligned} \quad (4)$$

$$\frac{\partial}{\partial t}(\rho Z) + \frac{1}{r} \frac{\partial}{\partial x}(\rho r u Z) + \frac{1}{r} \frac{\partial}{\partial r}(\rho r v Z) = \frac{1}{r} \frac{\partial}{\partial x} \left(\rho r \mathcal{D} \frac{\partial Z}{\partial x} \right) + \frac{1}{r} \frac{\partial}{\partial r} \left(\rho r \mathcal{D} \frac{\partial Z}{\partial r} \right) \quad (5)$$

Temperature and species profiles can be recovered from the conservation equation, Eq. (5). Denoting the variables over the flame front with the subscript f , it can be shown that the flame front position r_f , in the axial coordinate x is given by

$$Z_f = \frac{Y_{O_{A\infty}}}{\frac{W_{O\nu O}}{W_{F\nu F}} Y_{F_{F\infty}} + Y_{O_{A\infty}}} \quad (6)$$

On the fuel side of the flame the following expressions are used for the determination of temperature and species,

$$T = Z T_{F\infty} + \left(T_{A\infty} + Y_{O_{A\infty}} \frac{-h_{RP}}{c_p} \right) (1 - Z) \quad (7)$$

$$Y_F = Z Y_{F_{F\infty}} + Y_{O_{A\infty}} \frac{W_{F\nu F}}{W_{O\nu O}} (Z - 1) \quad (8)$$

$$Y_O = 0 \quad (9)$$

$$Y_P = Y_{O_{A\infty}} \frac{W_{P\nu P}}{W_{O\nu O}} (1 - Z) \quad (10)$$

$$Y_N = Y_{N_{A\infty}} (1 - Z) + Z Y_{N_{F\infty}} \quad (11)$$

and on the oxidizer side,

$$T = T_{A\infty} (1 - Z) + \left(T_{F\infty} + Y_{F_{F\infty}} \frac{-h_{RP}}{c_p} \right) Z \quad (12)$$

$$Y_F = 0 \quad (13)$$

$$Y_O = Y_{O_{A\infty}} (1 - Z) - Y_{F_{F\infty}} \frac{W_{O\nu O}}{W_{F\nu F}} Z \quad (14)$$

$$Y_P = \frac{W_{P\nu P}}{W_{F\nu F}} Y_{F_{F\infty}} Z \quad (15)$$

$$Y_N = Y_{N_{A\infty}} (1 - Z) + Z Y_{N_{F\infty}} \quad (16)$$

In the case of two products, i.e.,



species profiles are determined by

$$Y_{P_1} = \left(\frac{W_{P_1\nu_{P_1}}}{W_{P_1\nu_{P_1}} + W_{P_2\nu_{P_2}}} \right) Y_P \quad (18)$$

$$Y_{P_2} = \left(\frac{W_{P_2\nu_{P_2}}}{W_{P_1\nu_{P_1}} + W_{P_2\nu_{P_2}}} \right) Y_P \quad (19)$$

The variation of thermal properties with temperature is given by the following expressions,

$$\rho = \frac{\rho_0 T_0}{T} \quad (20)$$

$$\rho \mathcal{D} = \frac{\mu}{Pr_{ref}} \quad (21)$$

$$\mu = \mu_0 \left(\frac{T}{T_0} \right)^m \quad (22)$$

where $Pr_{ref} = 0.75$, $m = 0.7$ and $T_0 = 298$ K, $\mu = 1.85 \times 10^{-4}$ g/cm-s are reference values for air (Murty, 1975).

Following Xu and Smooke (1993), the heat release parameter $-h_{RP}/c_p$ is determined from an estimate peak temperature (T_{max}) (Norton *et al.*, 1993; Little, 2007),

$$\frac{-h_{RP}}{c_p} = \frac{1}{Y_{F_{F\infty}}} \left[\frac{T_{max} - T_{A\infty}(1 - Z_f)}{Z_f} - T_{F\infty} \right] \quad (23)$$

The considered system, based on the experiment of Mitchell *et al.* (1980), is presented in Fig. 1.

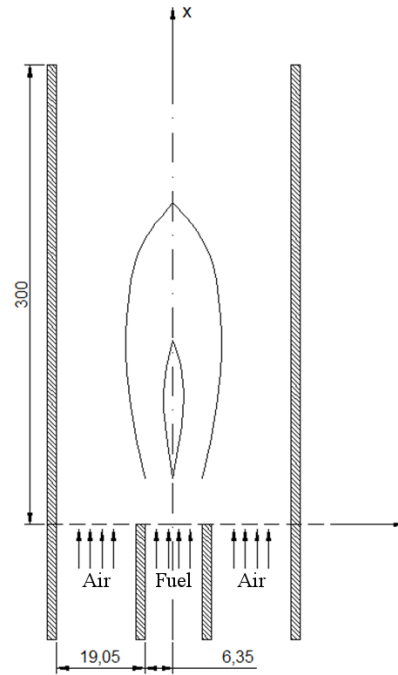


Figure 1. Schematic diagram of the axisymmetric burner (dimensions: mm).

3.1 Boundary and Initial Conditions

The computational domain in the co-flowing burner (Fig. 1) is enclosed by the inlet and exit in the axial direction, the symmetric centerline and the solid wall in the radial direction. The inlet of the burner is formed by an inner fuel jet and an outer air jet. Thus, the governing equations are subject to the following initial and boundary conditions,

$$\begin{cases} u = u_F, & v = 0, & Z = 1, & x = 0, & 0 < r < R_F & (24a) \\ u = u_O, & v = 0, & Z = 0, & x = 0, & R_F < r < R_O & (24b) \\ \frac{\partial u}{\partial x} = \frac{\partial v}{\partial x} = \frac{\partial Z}{\partial x} = 0, & P = P_0, & & x = L, & 0 < r < R_O & (24c) \\ \frac{\partial u}{\partial r} = v = \frac{\partial Z}{\partial r} = 0, & & & 0 < x < L, & r = 0 & (24d) \\ u = v = \frac{\partial Z}{\partial r}, & & & 0 < x < L, & r = R_O & (24e) \end{cases}$$

4. METHODOLOGY

A FORTRAN program was developed to obtain the numerical solutions. The conservation equations were discretized with the finite volume method. The physical domain was transformed to a computational one in order to consider a 80x80 nonuniform mesh. As the conservation equations are solved considering primitive variables, a method for the treatment of pressure-velocity coupling was necessary. The SIMPLEC method in a collocated mesh was used. Numerical solutions obtained for some classical cases were compared with analytical solutions for the verification of the program.

5. RESULTS

This section presents the obtained numerical results. The solution of the methane-air flame is compared with the experimental results of Mitchell *et al.* (1980). Ethanol-air flame profiles are compared to the methane-air flame.

5.1 Description of the Test Case

The test conditions employed are as follows:

Geometric Parameters

$$R_O = 2.54 \text{ cm}, R_F = 0.635 \text{ cm}, L = 30 \text{ cm}$$

Fuel Side

$$u_F = 4.5 \text{ cm/s}, v_F = 0 \text{ cm/s}, p = 1 \text{ atm}, T = 298 \text{ K}, Y_F = 1.0$$

Air Side

$$u_O = 9.88 \text{ cm/s}, v_O = 0 \text{ cm/s}, p = 1 \text{ atm}, T = 298 \text{ K}, Y_{O_2} = 0.232, Y_{N_2} = 0.768$$

5.2 Methane-Air Flame

The solution for the methane-air flame is obtained considering the following global irreversible infinitely fast reaction:



The profiles of the species and temperatures for three axial positions comparing the experimental results (Mitchell *et al.*, 1980) with the numerical solution obtained in the preset study are shown in Fig. 2, 3 and 4. The results show that the model captures the experimental results behavior. One observes that the solutions for CH_4 mass fractions have high discrepancy. This is due to model which considers Lewis number for all mixture components equals to one. Also, as noted by Xu and Smooke (1993) and Tarhan and Selçuk (2003) in a similar analysis, the model overestimates the flame height, which predicts some CH_4 mass fractions not observed by the experimental results (Fig. 3(a)). Because the penetration of oxidizer into the fuel side is not allowed in the flame-sheet model, the discrepancy of O_2 on the fuel side is due to this approximation. The higher H_2O concentration in the experimental data is caused by the moisture carried by the re-entrant flow from the exit due to recirculation in the burner Mitchell *et al.* (1980).

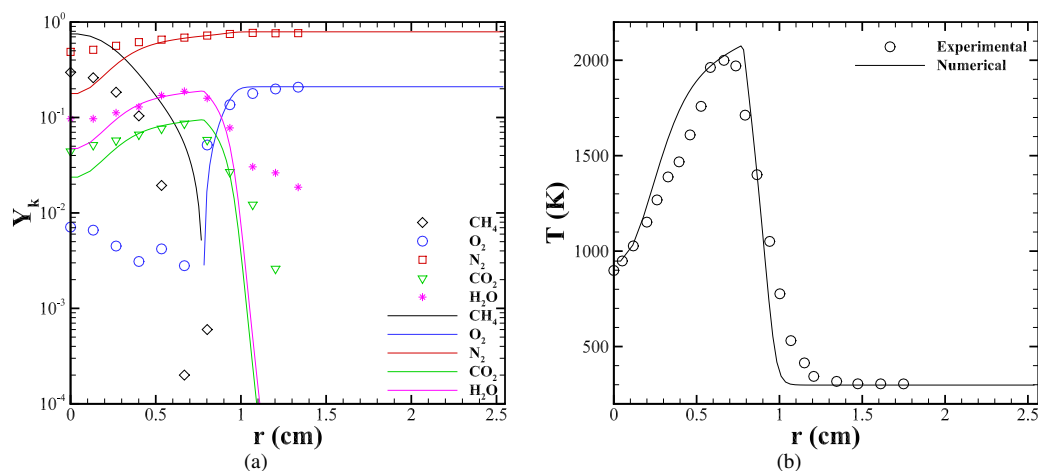


Figure 2. Comparison of profiles in $x = 1.2$ cm. (a) Mass fractions; (b) Temperature. Symbols: Mitchell *et al.* (1980).

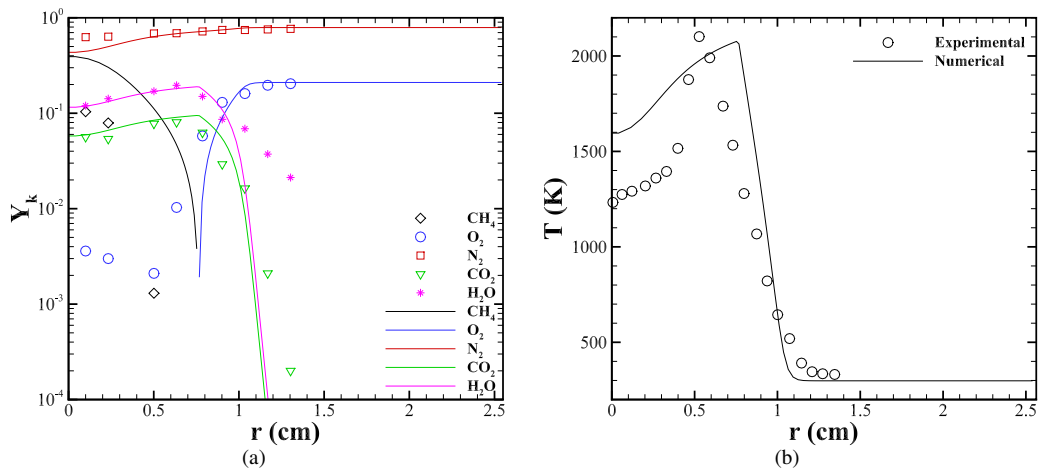


Figure 3. Comparison of profiles in $x = 2.4$ cm. (a) Mass fractions; (b) Temperature. Symbols: Mitchell *et al.* (1980).

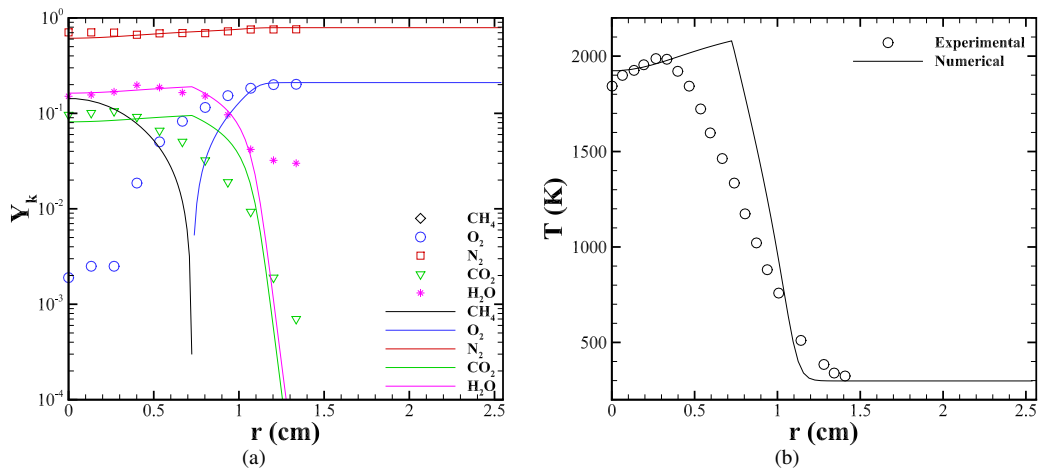


Figure 4. Comparison of profiles in $x = 5.0$ cm. (a) Mass fractions; (b) Temperature. Symbols: Mitchell *et al.* (1980).

The flame height can be defined as the height of the maximum temperature at the centerline (Mitchell *et al.*, 1980). The value obtained by the present study, 14 cm, is higher than the determined experimentally, 5.8 cm, as observed in Fig. 5. This is a common behavior of the flame sheet model (Xu and Smooke, 1993; Tarhan and Selçuk, 2003) and it is due to the use of infinitely fast reaction rates.

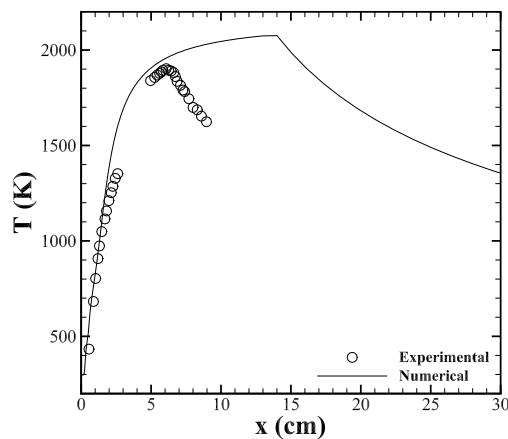
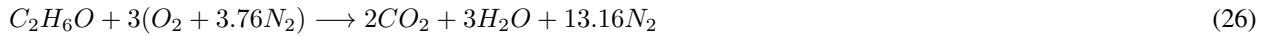


Figure 5. Comparison of temperature profiles along the centerline. Symbols: Mitchell *et al.* (1980).

The temperature solution presented shows reasonable agreement with the experimental results on the oxidizer side, being, nevertheless, able only to capture the temperature behavior on the fuel side. As the flame is located near to the centerline, better estimates are obtained near to the wall (air side). That peculiarity is due to the use of the flame sheet model, which overestimates temperature near to the flame.

5.3 Ethanol-Air Flame

The solution for the methane-air flame is obtained considering the following global irreversible infinitely fast reaction:



The profiles of temperature along the centerline determined numerically for methane and ethanol flames are shown in Fig. 6. The obtained flame height, defined as the height of the maximum temperature at the centerline, is 7.5 cm which may be, as mentioned, higher than the experimental value expected. The maximum temperature of both flames are very close, as expected due to Eq. (23) and the estimated values for the peak temperatures (Norton *et al.*, 1993; Little, 2007). Results also show that the methane flame is shorter than the flame obtained by the combustion of ethanol subjected to the same conditions. This is due to the difference between the rates of fuel to oxidizer mass.

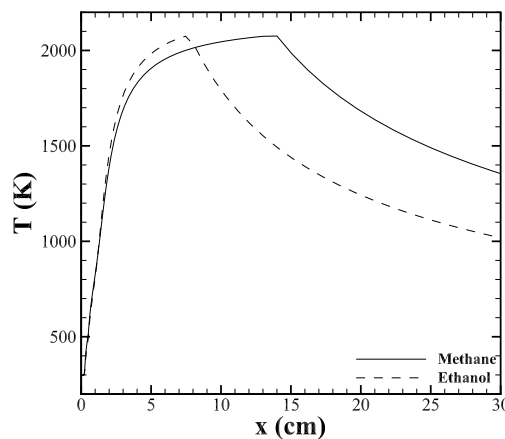


Figure 6. Comparison of temperature profiles along the centerline.

Methane and ethanol flames mixture fraction profiles are presented in Fig. 7. The flame position is shown by a white line. The different fuel to oxidizer mass rates of makes the ethanol flame shorter and thinner than the methane flame.

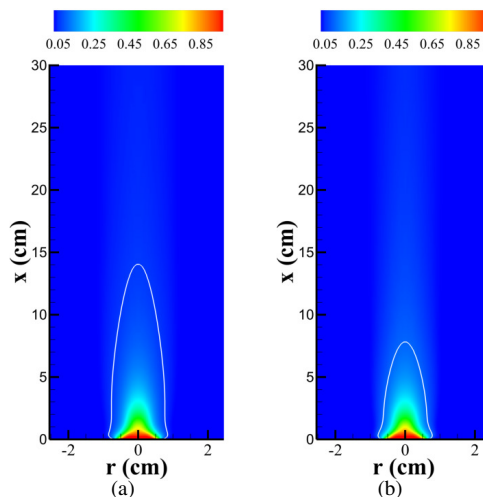


Figure 7. Comparison of mixture fraction profiles: (a) Methane flame; (b) Ethanol flame.

6. CONCLUSIONS

Results presented for the methane flame agree with experimental data (Mitchell *et al.*, 1980) despite the simplifications of the flame-sheet model. The main differences observed are due to the flame sheet model, which overestimates temperature near to the flame, which also modifies the species mass fractions profiles and the flame height. Results obtained for the ethanol flame represent well the expected behavior defined by the chemical reaction. The comparison between the methane and ethanol flames shows that the difference between the rates of fuel to oxidizer mass is determinant for the different structure obtained for each fuel. As the flame height is overestimated, the ethanol flame determined numerically should be higher than a flame. Thus, an experimental evaluation of the ethanol flame may be developed in order to validate the model and the results shown in the present work.

7. ACKNOWLEDGEMENTS

The authors would like to acknowledge the PRH-37 program of ANP for the grant that supported this study.

8. REFERENCES

- Burke, S.P. and Schumann, T.E.W., 1928. "Diffusion flames". *Industrial & Engineering Chemistry*, Vol. 20, No. 10, pp. 998–1004.
- Ern, A., Douglas, C.C. and Smooke, M.D., 1995. "Detailed chemistry modeling of laminar diffusion flames on parallel computers". *International Journal of High Performance Computing Applications*, Vol. 9, No. 3, pp. 167–186.
- Keyes, D.E. and Smooke, M.D., 1987. "Flame sheet starting estimates for counterflow diffusion flame problems". *Journal of Computational Physics*, Vol. 73, No. 2, pp. 267–288.
- Little, A.T., 2007. "Analysis of alternative fuel combustion in a perfectly stirred reactor".
- Lyu, H.Y. and Chen, L.D., 1991. "Numerical modeling of buoyant ethanol-air wick diffusion flames". *Combustion and Flame*, Vol. 87, No. 2, pp. 169–181.
- Mitchell, R., Sarofim, A. and Clomburg, L., 1980. "Experimental and numerical investigation of confined laminar diffusion flames". *Combustion and Flame*, Vol. 37, No. 0, pp. 227–244.
- Murty, K.A., 1975. *Introduction to Combustion Phenomena*. Gordon & Breach.
- Norton, T.S., Smyth, K.C., Miller, J.H. and Smooke, M.D., 1993. "Comparison of experimental and computed species concentration and temperature profiles in laminar, two-dimensional Methane/Air diffusion flames". *Combustion Science and Technology*, Vol. 90, No. 1-4, pp. 1–34.
- Saxena, P. and Williams, F.A., 2007. "Numerical and experimental studies of ethanol flames". *Proceedings of the Combustion Institute*, Vol. 31, No. 1, pp. 1149–1156.
- Tarhan, T. and Selçuk, N., 2003. "Numerical simulation of a confined Methane/Air laminar diffusion flame by the method of lines". *Turkish Journal of Engineering and Environmental Sciences*, Vol. 27, pp. 275–290.
- Uygun, A.B., Selçuk, N. and Tuncer, I.H., 2008. "A non-iterative pressure based scheme for the computation of reacting radiating flows". *International Journal of Thermal Sciences*, Vol. 47, No. 3, pp. 209–220.
- Uygun, A.B., Tarhan, T. and Selçuk, N., 2006. "Transient simulation of reacting radiating flows". *International Journal of Thermal Sciences*, Vol. 45, No. 10, pp. 969–976.
- Williams, F.A., 1994. *Combustion Theory: Second Edition*. Westview Press, second edition edition.
- Xu, Y. and Smooke, M.D., 1993. "Application of a primitive variable Newton's method for the calculation of an axisymmetric laminar diffusion flame". *Journal of Computational Physics*, Vol. 104, No. 1, pp. 99–109.

9. RESPONSIBILITY NOTICE

The authors are the only responsible for the printed material included in this paper.